Theoretical Fe $L_{2,3}$- and K-edge x-ray magnetic circular dichroism spectra of free iron clusters

Ondřej Šipr*
Institute of Physics, Academy of Sciences of the Czech Republic, Cukrovarnická 10, CZ-162 53 Prague, Czech Republic

Hubert Ebert†
Department Chemie, Universität München, Butenandtstrasse 5-13, D-81377 München, Germany
(Received 22 March 2005; revised manuscript received 15 August 2005; published 5 October 2005)

A fully relativistic *ab initio* theoretical scheme is employed for investigating $L_{2,3}$- and K-edge x-ray absorption near-edge structure (XANES) and x-ray magnetic circular dichroism (XMCD) spectra of free Fe clusters of 9–89 atoms. The $L_{2,3}$-edge spectra of clusters differ from spectra of bulk only quantitatively; a higher degree of localization of the d electrons in clusters is reflected through a higher intensity of the main XANES and XMCD peaks at the absorption edge. The K-edge XANES and XMCD spectra of clusters, on the other hand, differ from their bulk counterparts more significantly, even for the largest clusters investigated within our study. Several features, which could serve as spectroscopic markers of the difference between the clusters and bulk, were identified in both the $L_{2,3}$- and K-edge spectra. Contracting the bond lengths in clusters changes XMCD spectra only quantitatively.

DOI: 10.1103/PhysRevB.72.134406 PACS number(s): 75.50.Tt, 73.22.Dj, 78.70.Dm

I. INTRODUCTION

Clusters comprising from a few tens up to hundreds of atoms form an interesting class of materials, because they form a bridge between atoms and molecules on the one side and solids on the other side and yet their properties cannot be described by a simple interpolation between the two extremes. Magnetic properties of transition metal clusters, in particular, have attracted a lot of attention recently—both due to fundamental reasons and due to potential applications in magnetic recording technology. X-ray magnetic circular dichroism (XMCD), defined as the difference between the absorption rate for left- and right-circularly polarized x-rays in magnetic targets, $\Delta\mu=\mu^{(+)}-\mu^{(-)}$, is a frequently used tool for studying magnetism in clusters,[1–6] because it has several capabilities not supplied by other magnetic techniques (as, for example, chemical and angular momentum specificity).

The magnetic properties of transition metals (TM's) are determined mainly by their d electrons. Most XMCD studies of TM systems are therefore concerned with the $L_{2,3}$-edge spectra, which reflect properties of the d electrons due to the dipole selection rule. The spin magnetic moment μ_{spin} and the orbital magnetic moment μ_{orb} associated with the photoabsorbing atom can, under certain conditions, be extracted from XMCD spectra separately by applying a sum-rule analysis.[7–10] Low-lying d states are quite localized in TM's and, consequently, their $L_{2,3}$-edge spectra are rather atomiclike concerning their shape. The K-edge XMCD spectra, which probe the p electrons, are less frequently investigated in studies of TM magnetism. They carry information about the orbital polarization of states with p symmetry. The p-electron states are delocalized in TM's; therefore, the K-edge spectra have a more itinerant character. Due to that, $L_{2,3}$- and K-edge XMCD spectra offer complementary information.

So far, experimental investigations of the magnetism of free TM clusters have been mostly based on Stern-Gerlach-type measurements of deflection of their path in a magnetic field.[11,12] However, several XMCD measurements were performed on clusters supported by a substrate or embedded in a matrix. Studies of supported Fe clusters of a few hundreds to thousands of atoms[1–4] suggested a substantial enhancement of μ_{orb} as well as of the ratio $\mu_{\text{orb}}/\mu_{\text{spin}}$ with respect to the bulk. Similarly, XMCD experiments on small supported Fe clusters of just several atoms[5,6] suggested a strongly size-dependent μ_{orb}.

The properties of supported or embedded clusters are influenced both by cluster-specific effects and by cluster-substrate interactions; hence, they will differ from the properties of free clusters. Nevertheless, certain aspects of magnetism of one type of clusters can be elucidated by studying the other type. E.g., a recent theoretical study suggested that the magnetic properties of free Fe clusters and of Fe clusters supported by an inert substrate are similar to each other as the fraction of cluster atoms in direct contact with the substrate diminishes.[13] Generally, the present work is thus relevant also for clusters deposited on substrates with a weak interaction, such as graphite or semiconductors. Moreover, free clusters are interesting systems on their own, and while measuring XMCD in these systems would certainly be difficult, it could in principle be achieved with current or soon-to-be introduced experimental facilities. Note that x-ray absorption spectroscopy studies of size-selected free clusters were performed on several systems already.[14–16]

The aim of this study is to investigate theoretically $L_{2,3}$- and K-edge XMCD spectra of free Fe clusters of 9–89 atoms to explore their dependence on the cluster size and to compare them with the bulk spectra. The x-ray absorption near-edge structure (XANES) spectra of free clusters will be investigated as well, in order to offer a comprehensive view. As our main focus is on investigating the very basic effects connected with the finite cluster size, we restrict ourselves to nonrelaxed bulklike geometries. In real clusters, the effect of changing the cluster geometry and/or bond lengths will be superimposed on the effect of varying the cluster size. However, no definitive conclusions concerning the geometry of

free Fe clusters can be drawn from the studies published so far. There is experimental evidence for fcc[17] and icosahedral[18,19] as well as bcc geometries.[20,21] Theoretical studies of the ionization potentials of Fe clusters are consistent with bcc geometry.[22,23] *Ab initio* simulations suggest that small clusters (of less than 17 atoms) adopt various structures, with sometimes tiny differences in their total energies[24,25] (note that for a 15-atom cluster, the bcc geometry still cannot be ruled out).[24] On the other hand, for larger clusters theoretical modeling prefers structures which do not deviate too much from the basic bcc geometry.[26–28] Therefore, fixing the geometry of our clusters as bcc is a reasonable first guess.

We put the interatomic distances in the clusters same as in the bulk throughout most of this paper. On the one hand, this is certainly a simplification; on the other hand, given the fact that the "true" cluster geometry is still a matter of controversy, it is far from clear how the clusters should be deformed. By fixing the interatomic distances, we at least proceed along a well-defined direction and isolate the net effect of varying the cluster size. Note also that even without structure relaxation, calculating the magnetic properties of clusters is not without controversies (see, e.g., Fig. 3 of Ref. 29). However, as it would be useful to obtain a hint how the XMCD spectra of clusters may be affected by contraction of the bond lengths, we investigate this effect briefly as well.

The outline of the paper is the following: We start by introducing the systems we explore and by describing our theoretical approach. Then we briefly focus on XANES and XMCD spectra of bulk Fe crystal. The central part of this paper is formed by Secs. IV and V, where our results for the $L_{2,3}$- and K-edge XANES and XMCD spectra of clusters are presented in a greater detail. After that, we study how XMCD spectra of a 27-atom cluster are affected by contracting the bond lengths. We conclude by summarizing our main results.

II. COMPUTATIONAL METHOD

We investigate spherical-like clusters constructed from 1–7 coordination shells of bulk bcc Fe. Bulk interatomic distances are assumed (lattice constant $a=2.87$ Å), unless explicitly stated otherwise. Our calculations are based on the local spin density approximation (LSDA) scheme to deal with exchange and correlation effects. The Vosko-Wilk-Nusair parametrization of the exchange-correlation potential was used.[30] The reliance on the LSDA as opposed to the generalized gradient approximation (GGA) is justified in our study because we focus on magnetic properties of fixed-geometry systems. Although the GGA was found to be superior to the LSDA in exploring the structural properties of transition metals,[31] its benefit in magnetic studies is still questionable.[32–34]

In order to obtain XANES and XMCD spectra of clusters, one has to consider photoabsorption at each of their atomic sites and superpose all these individual spectra on top of each other. The spectra were calculated in real space via a fully relativistic spin-polarized multiple-scattering formalism within the atomic sphere approximation (ASA), using the SPRKKR code.[35,36] In order to account for the spilling of the electron charge into the vacuum, Fe clusters were surrounded by empty spheres. The scattering potential was obtained from self-consistent-field (SCF) calculations using an amended XASCF code.[37–39] A more detailed description of our theoretical approach as well as calculated site-dependent magnetic moments in the clusters can be found in our previous work.[29] Some more technical information about calculating XMCD spectra in clusters and about their site and size dependence in general can be found in Ref. 39.

The helicity of the incoming photons is assumed to be either parallel or antiparallel with cluster magnetization $\boldsymbol{M}$ throughout this study. All results presented here correspond to the case when the direction of $\boldsymbol{M}$ coincides with the [001] direction of the underlying bcc crystal lattice. This might seem a restriction, because magnetic properties in general depend on the direction of $\boldsymbol{M}$ due to the spin-orbit interaction. Dependence of μ_{orb} on $\boldsymbol{M}$ may serve as a quick estimate of this anisotropy.[40] Our earlier study demonstrated that although μ_{orb} at individual atoms of bcc-like Fe clusters indeed varies if the direction of $\boldsymbol{M}$ changes,[29] the *average* μ_{orb} over all atoms of the cluster, on the other hand, practically does not depend on the orientation of $\boldsymbol{M}$. As the total XANES and XMCD spectra of clusters represent averages over individual spectra of all the atoms, one can expect that their dependence on $\boldsymbol{M}$ can be estimated from the *average* μ_{orb} rather than from μ_{orb}'s at individual atoms. That means that the spectra should not significantly depend on the orientation of $\boldsymbol{M}$. We verified this conjecture by direct calculations: if $\boldsymbol{M}$ is oriented along the [110], [111], and [211] directions, the spectra practically coincide with the spectra obtained for $\boldsymbol{M}$ along the [001] direction. Our results are therefore quite general in this respect. Note that we assume, nevertheless, that the direction of the incoming photon is always parallel to $\boldsymbol{M}$. The dependence of XMCD spectra on the angle between the photon helicity and $\boldsymbol{M}$ was investigated, for example, by Fujikawa and Nagamatsu.[41,42] For systems with a mirror symmetry (which applies here), the XMCD intensity is just proportional to the cosinus of the angle between $\boldsymbol{M}$ and the photon beam direction.[41]

A core hole is created during the x-ray absorption process, which dynamically modifies the unoccupied states seen by the excited photoelectron. In order to deal with this effect properly, one would have to go beyond the LSDA. An approximative treatment of the core hole is possible within the LSDA relying on the so-called final-state rule.[43,44] Other LSDA-based approaches to account for various aspects of the core hole include the consideration of relaxation and screening by various other, sometimes rather semiempirical, procedures.[45–47] In this work we do not take the presence of the core hole into account; i.e., our calculations correspond to the ground state. This is partly justified by earlier work which found that including the core hole in a static way does not influence the calculated $L_{2,3}$- and K-edge XMCD spectra of bulk Fe in a substantial way,[48,49] partly by the fact that serious doubts can be raised about the ability of the LSDA to describe conduction-electron relaxation in magnetic materials in principle.[50] More sophisticated as well as more laborious methods would have to be employed for an adequate treatment of the core hole in this case.[51–54] As one can assume that the core-hole effect in a Fe crystal and in Fe clus-

ters will not be dramatically different, its neglect is reasonable in this study.

All calculated raw spectra were convoluted by a Lorentzian curve in order to simulate the effect of a finite core-hole lifetime.[55] We included also a Gaussian broadening to mimic the experimental resolution (0.20 eV at the L edges and 0.80 eV at the K edge). An additional broadening which should account for a finite photoelectron lifetime should be further applied on top of that. The exact form of this broadening is not known, as it is governed by complex many-body processes, which cannot be described within the plain LSDA scheme. Generally, either one can estimate this broadening by interpolating known experimental data[56] or one can fit it within certain constraints in order to match the shape of the experimental spectrum.[57] In this work we adopted the second approach and chose the broadening associated with the photoelectron lifetime by amending the "universal curve" of Müller *et al.*[56] according to the suggestions of Ref. 57, so that a reasonable overall agreement between theoretical and experimental bulk spectra is achieved. In that way, we can concentrate on significant spectral features and smear out most of the faint details when comparing bulk and cluster spectra in Secs. IV and V. An alternative way of incorporating the photoelectron decay would be employing a complex (energy-dependent) optical potential.[58,59]

III. SPECTRA OF A BULK Fe CRYSTAL

Prior to dealing with spectra of clusters, we focus briefly on XANES and XMCD spectra of a Fe crystal and compare our calculations with earlier experimental and theoretical work. Apart from verifying the adequacy of our theoretical approach, this section provides us with a reasonable estimate of the energy-dependent broadening function which is supposed to account for the decay of the excited photoelectron (see the end of Sec. II). Contrary to the rest of this paper, the spectra presented in this section were obtained via a *reciprocal*-space calculation, unless explicitly stated otherwise [see Ref. 36 for a more detailed description of the relativistic Korringa-Kohn-Rostoker (KKR) method applied to bulk systems].

A. $L_{2,3}$-edge spectra of a crystal

We start presenting our results for the $L_{2,3}$-edge spectra because these spectra are usually in focus when investigating TM magnetism. The upper panel of Fig. 1 compares the experimental $L_{2,3}$-edge XANES spectrum of a Fe crystal taken from Ref. 60 with our calculated spectrum, while the lower panel of Fig. 1 shows the corresponding XMCD spectra. The experimental and theoretical XANES curves were vertically aligned to each other so that they have the same intensity in the high-energy tail; the XMCD spectra were aligned accordingly (i.e., scaled by the same factor as the XANES spectra). This way of aligning theoretical and experimental spectra may not always produce the best apparent agreement due to problems with background subtraction. Nevertheless, it is frequently employed in x-ray absorption spectroscopy studies. Absolute units (megabarns) on the vertical axes of Fig. 1

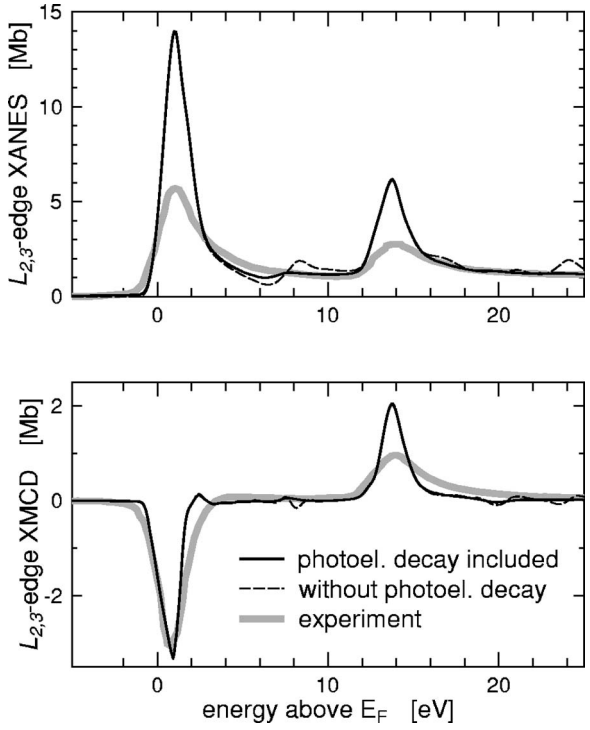

FIG. 1. Calculated $L_{2,3}$-edge spectra of Fe crystal compared to experiment of Chen *et al.* (Ref. 60). The upper panel shows x-ray absorption spectra; the lower panel shows XMCD spectra. Theoretical spectra are displayed either without accounting for the photoelectron-lifetime-related broadening (thin dashed lines) or including it (thin solid lines). Experimental curves are represented by thick lines.

were supplied by the calculation—the experimental spectra were provided in a relative scale only.[60] Our theoretical spectra were broadened in a twofold way. In the first case, only the effects of the finite core-hole lifetime and of the experimental resolution were considered; i.e., the photoelectron decay was ignored (thin dashed lines in Fig. 1). In the second case, we applied an additional photoelectron-lifetime-related broadening optimized so that it yields the best overall shape of the $L_{2,3}$- and K-edge XANES and XMCD crystalline spectra (thin solid lines in Fig. 1).

Our calculated $L_{2,3}$-edge spectra are similar to those obtained by other authors.[50,61–63] Most of the differences between various calculations stem most probably from a different amount of broadening applied in different investigations, which is decided only on a semiempirical basis usually.

One can see from Fig. 1 that the ratio of the intensities of the L_2 and L_3 white lines is not reproduced very accurately. This ratio is affected by the presence of the core hole in the experiment.[52,54] A static theoretical scheme cannot account for this effect properly. However, one can assume in the first approximation that it would not be very different in clusters and in the bulk, meaning that our ability to compare spectra of clusters and of the bulk is not seriously affected by this.

There is no clear experimental counterpart in Fig. 1 to the small theoretical XANES peak at ~8 eV. This peak occurs in other theoretical studies as well[50,61–63] and has been ascribed to a van Hove singularity.[64] A shoulder can be seen in

some experimental spectra of Fe/Cu(100) multilayers around this energy[65] but is absent in other spectra of Fe multilayers.[66] So there is a possibility that this peak is usually smeared out by inelastic processes but nevertheless can be observed under certain conditions.

B. *K*-edge spectra of a crystal

Theoretical and experimental *K*-edge XANES spectra are displayed in the upper panel of Fig. 2; XMCD spectra are shown in the lower panel. The lower half of each panel is analogous to Fig. 1: one theoretical curve includes the broadening related to the photoelectron decay (thin solid line), while the other theoretical curve omits it (dashed line). The experimental data were taken from the work of Pizzini *et al.*,[67] again scaled so that the XANES intensity agrees with the theoretical curve at high energies (see the beginning of Sec. III A). Our calculated XANES spectrum agrees quite well with the experiment, while the agreement of XMCD spectra is less satisfactory—the positions of all the XMCD peaks except for the first one ought to be shifted more or less uniformly by 2 eV to higher energies.

Several earlier calculations of the *K*-edge XMCD spectra of Fe crystal exist.[42,49,59,68–73] As an illustration, we compare our data with the real-space calculations of Brouder *et al.*,[49] because they focus on a similar energy range as we do. Their results are shown by dot-dashed lines in the upper half of both panels of Fig. 2. It appears that calculations of Brouder *et al.*[49] describe the XMCD spectra better than our calculations; on the other hand, the XANES spectrum is described better in this work than by the calculations of Brouder *et al.*[49] It is not quite clear what the reason is for these differences. Apart from a different treatment of the spin-orbit coupling (fully relativistic formalism in this work, the perturbative treatment in Ref. 49), both studies use similar techniques and approximations. In both cases, a self-consistent potential subject to a similar shape approximation is used (Brouder *et al.*[49] obtained it relying on a linear combination of muffin-tin orbital method).[74] We checked that the finite size of the cluster employed by Brouder *et al.*[49] (259 atoms) is not a factor: our own real-space calculation for the same cluster size agrees with our reciprocal-space results quite accurately (long-dashed lines in the upper half of both panels of Fig. 2—we display only the case when broadening due to photoelectron decay was ignored). Note that the real-space calculation of ours involves a potential taken from the reciprocal-space calculation for an infinite crystal; i.e., the same potential was employed for obtaining all the spectra presented in Sec. III. The different choice of exchange-correlation potential cannot explain the difference in spectra either, as we checked that using the von Barth-Hedin potential[75] (used by Brouder *et al.*) instead of the Vosko-Wilk-Nusair[30] parametrization shifts the peak positions by 0.1 eV at most.

The peak around 10 eV in the XMCD spectrum is too intensive in our calculations as well as in several other calculations.[49,59,69] Its intensity seems to be better reproduced by calculations of Fujikawa and Nagamatsu;[42] however, their approach does not reproduce the intensity of the first peak at 1 eV accurately (see Fig. 9 of Ref. 42).

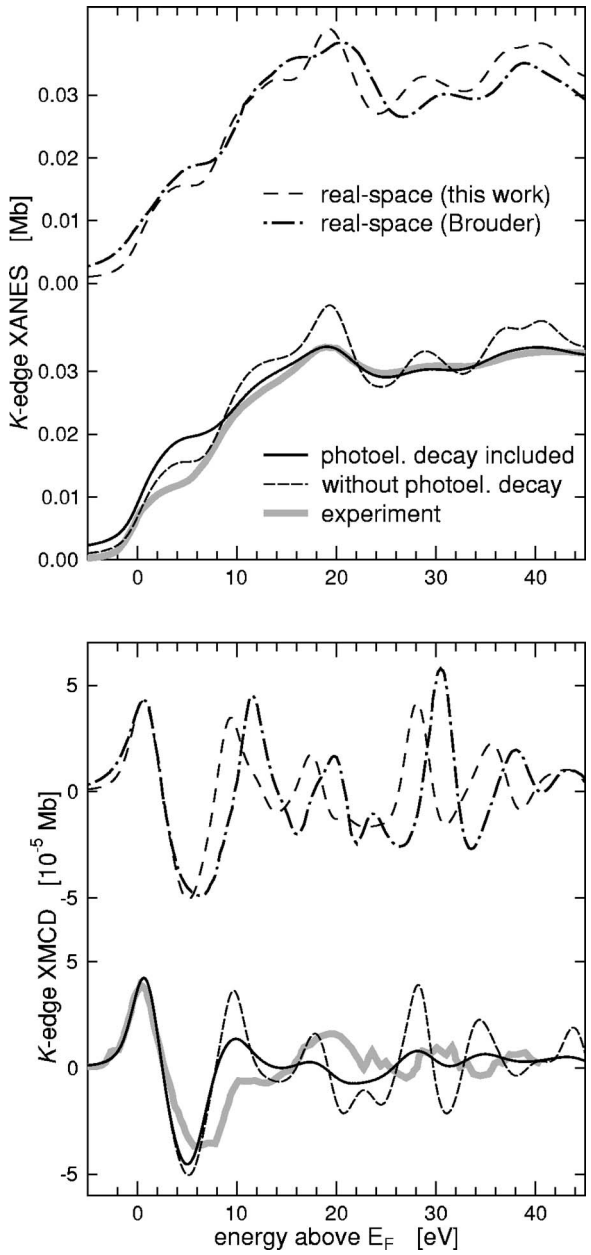

FIG. 2. Theoretical *K*-edge spectra of Fe crystal compared to experiment. The upper panel shows x-ray absorption spectra; the lower panel shows XMCD spectra. The upper half of each panel displays our real-space calculation (long-dashed lines) together with the real-space calculation of Brouder *et al.* (Ref. 49) (dotted-dashed lines). The lower half of each panel displays spectra calculated in a reciprocal space, together with experimental results of Pizzini *et al.* (Ref. 67) (thick lines). Our spectra were calculated either without accounting for the photoelectron-lifetime-related broadening (short- and long-dashed lines) or including it (thin solid lines).

In spite of the various differences, all the calculations nevertheless agree with one another on the gross features and trends of the $L_{2,3}$-edge as well as of the *K*-edge XMCD spectra. To conclude this part, we note that the agreement of our bulk Fe $L_{2,3}$- and *K*-edge XANES and XMCD calculations with the experiment is satisfying enough to make the mutual

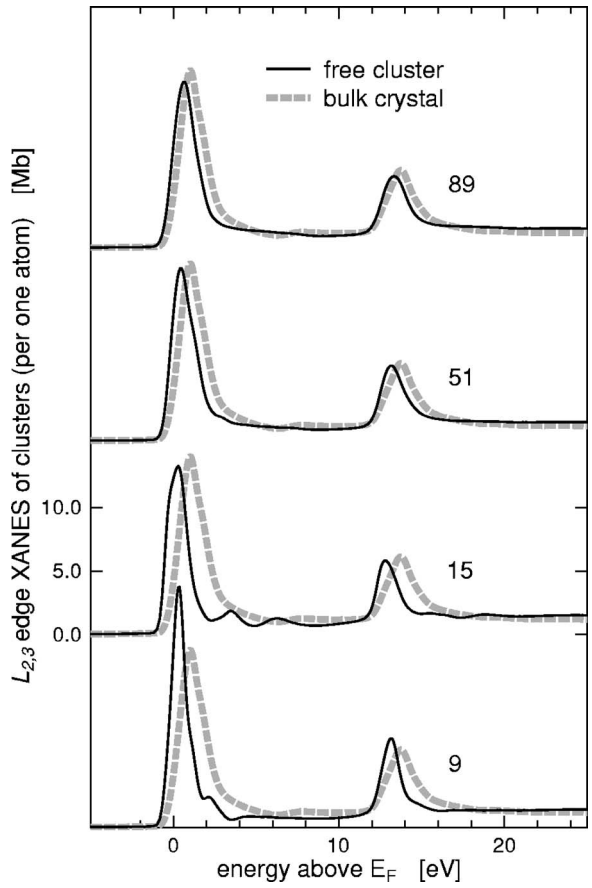

FIG. 3. Calculated $L_{2,3}$-edge XANES of free clusters (thin solid line) compared to theoretical XANES of a crystal (thick dashed line). The number of atoms in the cluster is shown in each graph. Note that the curve representing the crystal XANES is the same in each of the four graphs.

comparison of bulk and cluster spectra done in the following section meaningful.

IV. $L_{2,3}$-EDGE SPECTRA OF CLUSTERS

We calculated the XANES and XMCD spectra of Fe clusters comprising 9, 15, 27, 51, 59, 65, and 89 atoms. The signals originating from each of the atoms of a given cluster were superposed in order to yield the total spectrum of the whole cluster. Moreover, the spectra obtained in this way were divided by the number of atoms in the cluster in order to provide a common normalization. In this section (as well as in Sec. V), the broadening of the raw theoretical data includes the effect of the finite photoelectron lifetime.

Figure 3 displays the $L_{2,3}$-edge XANES spectra of free clusters and compares them to the spectrum of a crystal. As XANES is not in the focus of this study, only results for four representative cluster sizes were selected. One can see from Fig. 3 that the spectra do not display significant variations with cluster size, except for some fine structure just after the L_3 white line in the case of the 9- and 15-atom clusters ($E \approx 2-6$ eV). This additional fine structure may be connected with the fact that we are actually dealing with truly discrete states below the vacuum level. The height of the vacuum level with respect to E_F increases from 5 eV for the 9-atom cluster to 8 eV for the 89-atom cluster; this trend is in agreement with previous tight-binding model Hamiltonian calculations.[22] The continuous character of x-ray absorption spectra in the region below the vacuum edge results mathematically from the Green function formalism we employ for energies with a small imaginary part and physically from lifetime broadening processes. When the cluster size increases, the number of discrete levels increases as well, which leads to a smoothening of the spectral peaks (due to their mutual overlap) and to a generally larger width of the resulting "band." Consequently, the white lines for small clusters are much sharper than the white lines for larger clusters, as is also evident from Fig. 3. Interestingly, the vacuum edge itself apparently does not give rise to a step in the absorption spectra.

Another feature characteristic for XANES of clusters is the absence of the small hump at 8 eV. As we mentioned above (Sec. III A), this peak appears in the theoretical spectrum of Fe crystal and is related to a van Hove singularity. That means that its existence is closely connected with the translational periodicity and can thus evolve only in sufficiently large systems. This conclusion is supported by an earlier study of Fe clusters cut from the bulk (i.e., with bulk potentials at each site), where an analogous feature appears in XMCD of atoms in the center of clusters only if they contain more than ~ 100 atoms.[39]

Theoretical $L_{2,3}$-edge XMCD spectra are shown in Fig. 4 for all cluster sizes we investigated. One can see that the general shape of the XMCD curves for the clusters and for the bulk is quite similar—the spectra are dominated by two main peaks, with little fine structure apart from them. The peak intensity systematically decreases with increasing cluster size. Another systematic trend concerns the peak widths: the smaller clusters provide more narrow XMCD peaks than the larger clusters (the full width at half maximum of the L_3 peak rises from 1.0 eV for a 9-atom cluster to 1.1 eV for a 51-atom cluster to 1.3 eV for a 89-atom cluster). These trends in XMCD spectra can be viewed as counterparts to analogous trends in the XANES spectra; they are connected with a higher degree of localization of the d electrons in small clusters.

For each cluster size a small yet distinct positive hump appears just after the main L_3 peak ($1-2$ eV above E_F). This feature appears in the calculated XMCD of a Fe crystal as well but it is much less intensive in that case. There is also a small change in the shape of the main XMCD peaks in the clusters as compared to the bulk: in the clusters, these peaks are steeper on the low-energy side while in the bulk the peaks are more symmetric.

The height of XMCD peaks decreases with increasing cluster size nearly monotonously. This trend seems to reflect the gradual change of the character of the electron d states from atomiclike to bulklike when the cluster size increases. On the other hand, the areas of $L_{2,3}$-edge XMCD peaks do not follow any simple trend. This is not really surprising because these areas should reflect the cluster magnetization,[7,9,10] which oscillates with cluster size. One can see this from Table I which summarizes some calculated mag-

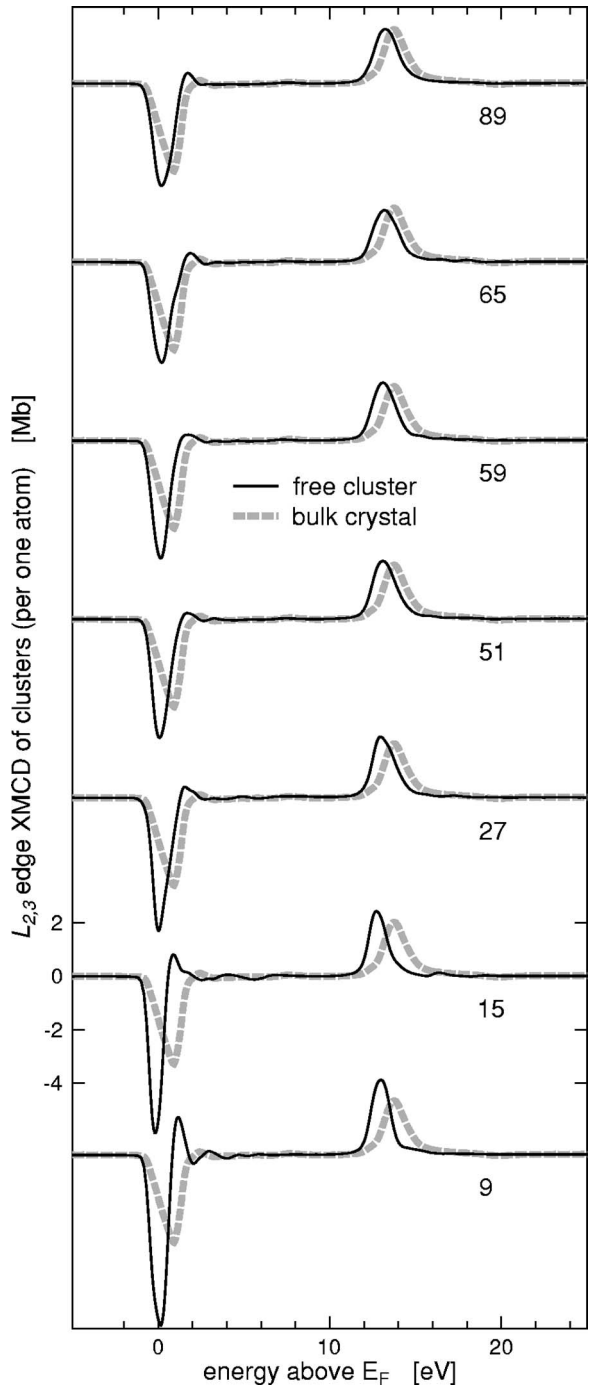

FIG. 4. Calculated $L_{2,3}$-edge XMCD of free clusters (thin solid line) compared to theoretical XMCD of a crystal (thick dashed line). The number of atoms in the cluster is shown in each graph.

netic properties of our clusters (see Ref. 29 for local magnetic moments from which this table was assembled). Theoretical results for bulk Fe crystal are also shown for comparison. A more quantitative analysis in terms of the sum rules would require a proper consideration of the magnetic dipole term T_z because it could be significant for atoms in the outer shells.[76] As the T_z term was not calculated in this study, no definite assessment of the applicability of sum rules in clusters can be done.

TABLE I. Magnetic properties of free iron clusters averaged over all their atoms as a function of cluster size. The first column displays the number of atoms in a cluster, the second column shows the average d component of the spin magnetic moment $\mu_{\mathrm{spin}}^{(d)}$, the third column shows the average number of holes in the d band $n_h^{(d)}$, the fourth column shows the average of ratios $\mu_{\mathrm{spin}}^{(d)}/n_h^{(d)}$, the fifth column contains the average d component of the orbital magnetic moment $\mu_{\mathrm{orb}}^{(d)}$, and the last column contains the average p component of the orbital magnetic moment $\mu_{\mathrm{orb}}^{(p)}$. Magnetic moments are in μ_B.

Size	$\mu_{\mathrm{spin}}^{(d)}$	$n_h^{(d)}$	$\mu_{\mathrm{spin}}^{(d)}/n_h^{(d)}$	$\mu_{\mathrm{orb}}^{(d)}$	$\mu_{\mathrm{orb}}^{(p)}$
9	2.84	3.36	0.838	0.209	−0.00177
15	2.54	3.15	0.814	0.071	−0.00088
27	2.82	3.40	0.823	0.125	−0.00027
51	2.62	3.36	0.784	0.075	0.00009
59	2.67	3.35	0.800	0.063	−0.00014
65	2.65	3.38	0.788	0.075	−0.00055
89	2.68	3.48	0.771	0.068	0.00003
bulk	2.37	3.44	0.689	0.055	0.00006

Neither μ_{spin} nor μ_{orb} approaches bulk values even for the 89-atom cluster. This is not surprising: the total magnetic moment in free clusters converges to the bulk value only for clusters containing several hundreds of atoms.[11] The average spin and orbital magnetic moments of Table I strongly oscillate with cluster size for clusters of less than 27 atoms. Oscillations of similar amplitude appear in average μ_{spin} and μ_{orb} of *supported* Fe clusters of 2–9 atoms, as derived from XMCD measurement.[6] On the other hand, the model tight-binding calculations of Martínez *et al.*[77] for 2–9 iron atoms deposited on a substrate predict only a mild variation of average magnetization with number of atoms. In view of our results, the large oscillations observed by Lau *et al.*[6] seem more plausible than the gradual change of μ_{spin} found by Martínez *et al.*[77]

XMCD experiments on supported Fe clusters suggest that the ratio $\mu_{\mathrm{orb}}/\mu_{\mathrm{spin}}$ should be about twice as large in those systems as in a Fe crystal.[1–3] On the other hand, it follows from Table I that this ratio is 0.023 for a Fe crystal and 0.025 for an 89-atom cluster, which means only a 10% increase. The cause of this discrepancy may be that the supported clusters are more flat than spherical, containing thus a much larger portion of surface and edge atoms with larger μ_{orb}.

XMCD spectra of whole clusters, shown in Fig. 4, were obtained by superposing spectra originated at each of the individual atoms in the cluster. These individual spectra are displayed separately in Fig. 5 for the 27-atom cluster (see our earlier preliminary report[78] for a few more examples). Not surprisingly, spectra at L edges of atoms belonging to different coordination shells differ from one another. Moreover, atoms which belong to the same coordination sphere but are inequivalent due to the lowering of the symmetry by the spin-orbit coupling[79] give rise to different XMCD spectra as well (these atoms are distinguished in Fig. 5 as belonging either to the group which contains the majority of atoms of the given shell or to the group comprised of the minority of

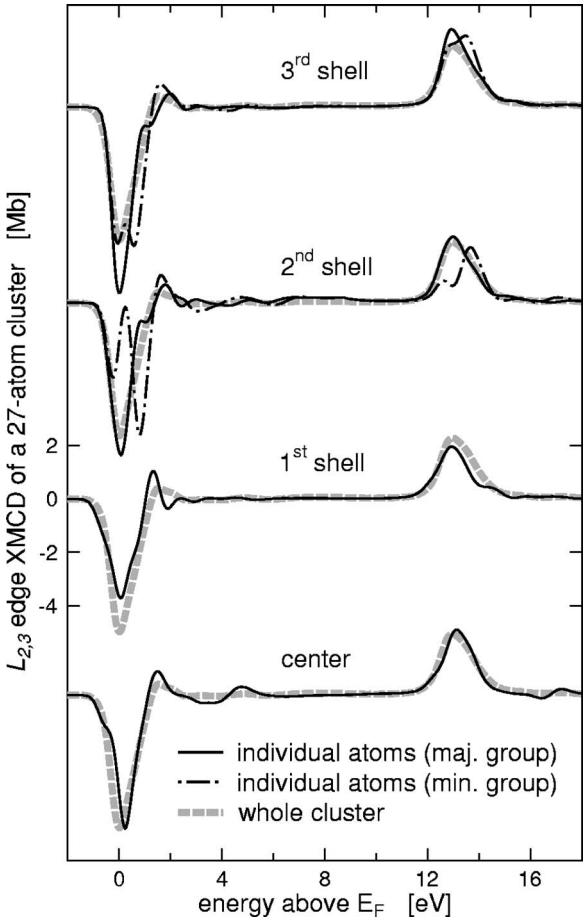

FIG. 5. Calculated $L_{2,3}$-edge XMCD spectra of individual atoms in a 27-atom cluster. Each graph is devoted to atoms of one coordination shell. Spectra of atoms belonging to the same coordination shell which are nonetheless inequivalent due to the presence of magnetization and spin-orbit coupling are distinguished by line types (solid lines for atoms of the majority group, dash-dotted lines for atoms of the minority group). The spectrum of the whole cluster (normalized to one atom) is shown by a thick dashed line in each graph for comparison.

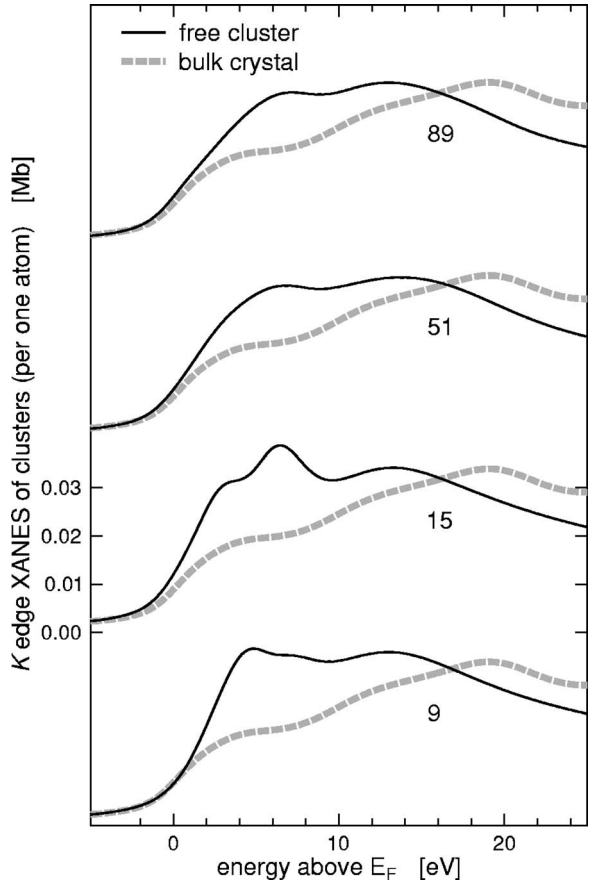

FIG. 6. Calculated K edge XANES of free clusters (thin solid line) compared to theoretical XANES of a crystal (thick dashed line). The number of atoms in the cluster is shown in each graph.

such atoms). One can see that XMCD spectra of atoms which would be symmetry equivalent in the absence of spin-orbit coupling differ sometimes quite significantly. This effect can be seen as an analogy to the fact that μ_{orb} may also vary significantly for such atoms.[29] This analogy may go even further: It was shown[29] that although μ_{orb} at inequivalent atoms of the same coordination shell in a bcc Fe cluster depends on the direction of $\boldsymbol{M}$ significantly, the average value of μ_{orb} practically does not depend on $\boldsymbol{M}$. That can be viewed as a counterpart to the negligible dependence of XMCD spectra of clusters (which arise by *averaging* the spectra of individual atoms) on the direction of $\boldsymbol{M}$ we mentioned in Sec. II.

Figure 5 also demonstrates that our finding that $L_{2,3}$-edge XMCD spectra of Fe clusters differ from their bulk counterpart only quantitatively does not contradict earlier calculations which found that the main peaks actually split into two in XMCD of Fe crystal surface[61] and of Fe multilayers.[80] A similar peak splitting can be observed in the calculated spectra of some individual atoms (see the second from the top graph of Fig. 5). However, when forming the total spectrum of the whole cluster, fine-structure contributions arising from inequivalent atomic sites cancel each other and hence the total XMCD signal does not exhibit them.

In general, one observes that the $L_{2,3}$-edge XANES and XMCD spectra of Fe clusters differ from the bulk spectra only quantitatively. This can be intuitively understood as a manifestation of the essentially local character of the d-electron states which are probed by the $L_{2,3}$-edge spectra in TM's. Interestingly, the difference between clusters and the bulk is more significant in XMCD than in XANES.

V. K-EDGE SPECTRA OF CLUSTERS

K-edge XMCD spectra reflect the orbital polarization of unoccupied p states, which is quite a subtle effect in TM's.[70] On the other hand, the p electrons are highly delocalized in these systems and hence one can expect that the finite size of the clusters will influence the K-edge spectra more significantly than in the case of the $L_{2,3}$-edge spectra stemming from more localized d electrons.

Theoretical XANES of selected free clusters is compared with XANES of a crystal in Fig. 6. As anticipated, the difference between spectra of clusters and of the bulk is now

significantly larger than it was in the case of the $L_{2,3}$-edge spectra (see Fig. 3). As a general rule one observes from Fig. 6 that small clusters give rise to XANES spectra with higher intensities in the low-energy lobe of the main peak than spectra of larger clusters. Differences in the fine structure of this main peak can be observed as well. Even for the largest cluster investigated (89 atoms), the difference between cluster and bulk XANES appears to be quite significant.

Our main emphasis is laid on the XMCD spectra, however. Theoretical *K*-edge XMCD spectra of clusters and of a crystal are displayed in Fig. 7. One can observe that the spectra of clusters differ quite significantly from the bulk spectrum. The size of the clusters affects not only the shape and intensity of individual oscillations but also their positions—especially for the small clusters. A particular feature worth mentioning is the suppression of the first positive peak around 1 eV for quite a broad range of cluster sizes. It is clear that the *K*-edge XMCD is significantly more sensitive to the cluster geometry and size than the $L_{2,3}$-edge XMCD.

By comparing Figs. 3 and 4 with Figs. 6 and 7, one can see that the finite cluster size affects the spectra in a different way at the $L_{2,3}$ edge and at the *K* edge. This reflects the different nature of low-lying unoccupied *d* and *p* states. The *d* states are quasilocalized, and the dominant $L_{2,3}$-edge spectral features in TM's are essentially atomic like, meaning that their shapes only mildly depend on the local geometry around the photoabsorbing atoms. Consequently, varying the cluster size affects the $L_{2,3}$-edge spectral shapes only indirectly, by changing the degree of localization of the *d* states. The $L_{2,3}$-edge spectra of different clusters are therefore quite similar one to another, and the relatively small change of spectra caused by varying the localization of the *d* states thus can get revealed. On the other hand, unoccupied *p* states are extended in their nature, implying that changes in the cluster geometry or size by adding another coordination shell will have significant influence on the shape of *K*-edge spectra. Any possible systematic trends induced by changes of the localization of the *p* states in free clusters are thus overridden by more significant effects which are directly related to changes of the local neighborhood of photoabsorbing atoms.

The *K*-edge XMCD spectra cannot serve as a suitable measure of integral magnetic quantities in clusters (such as magnetic moments). Namely, the *K*-edge XMCD of TM's cannot be unambiguously interpreted in terms of integral sum rules because one cannot easily separate photoelectron transitions to the 4*p* states from transitions to other shells[70,81] (unlike in the case of the $L_{2,3}$-edge spectra, where the white lines can be almost exclusively ascribed to transitions to the 3*d* states). One has to resort to the differential form of the sum rules in order to obtain an intuitive interpretation of the *K*-edge XMCD signal as a measure of the *p* component of the orbital polarization of the unoccupied states.[82] Nevertheless, for the sake of completeness we present in the last column of Table I the average *p* component of μ_{orb} for all the clusters we studied. This quantity oscillates with cluster size (not only in magnitude but in sign as well), which can be viewed as yet another indication that no systematic unidirectional trend in the *K*-edge XMCD spectra of Fe clusters as a function of their size can be expected.

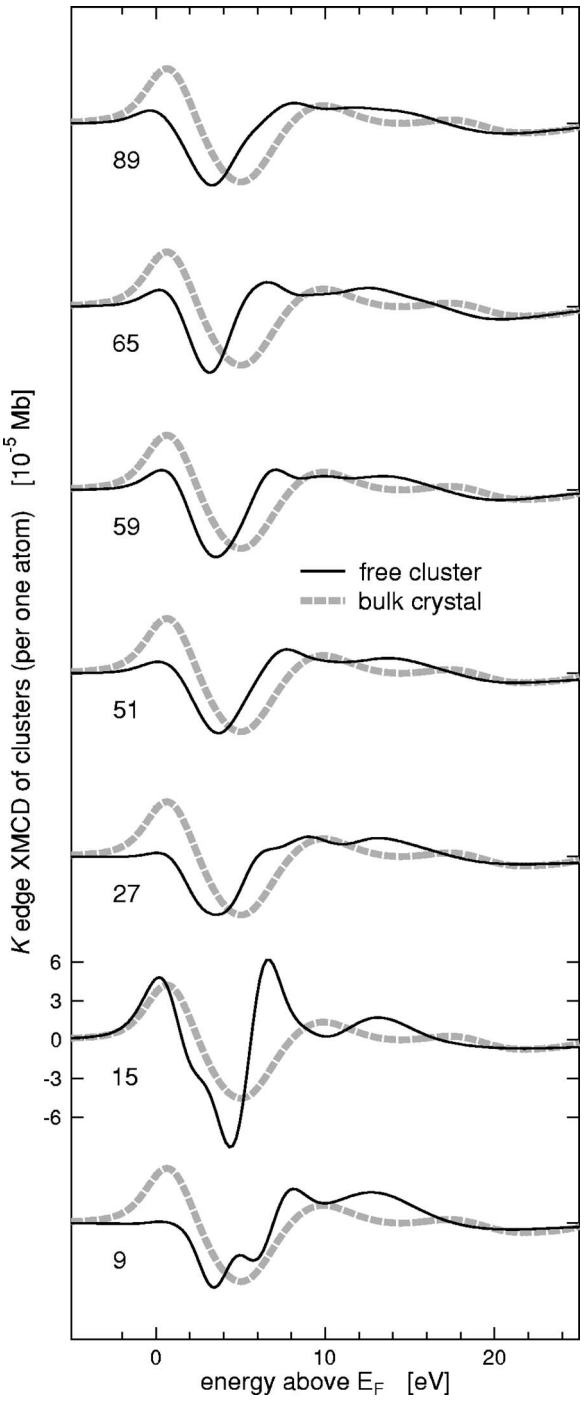

FIG. 7. Calculated *K*-edge XMCD of free clusters (thin solid line) compared to theoretical XMCD of a crystal (thick dashed line). The number of atoms in the cluster is shown in each graph.

Figure 8 compares the XMCD spectrum of the whole 27-atom cluster with spectra arising from individual atoms of this cluster. Similarly as in the case of the $L_{2,3}$ edge, one can see that there is a considerable variation among the individual spectra. The decrease of symmetry due to magnetization and spin-orbit coupling means that *K*-edge XMCD spectra of otherwise equivalent atoms differ from one another, similarly as in the case of the $L_{2,3}$-edge XMCD (compare

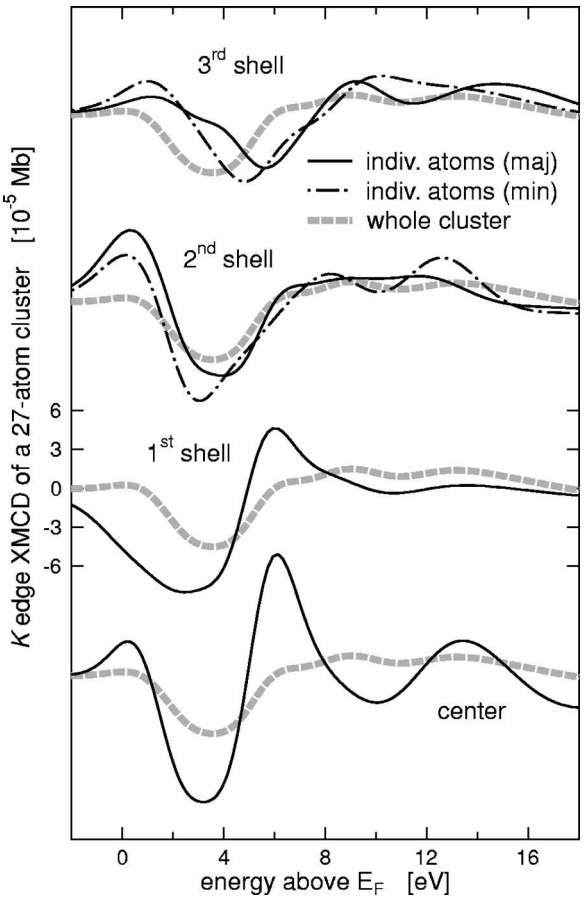

FIG. 8. Calculated K-edge XMCD spectra of individual atoms in a 27-atom cluster. The meaning of the lines is the same as in Fig. 5.

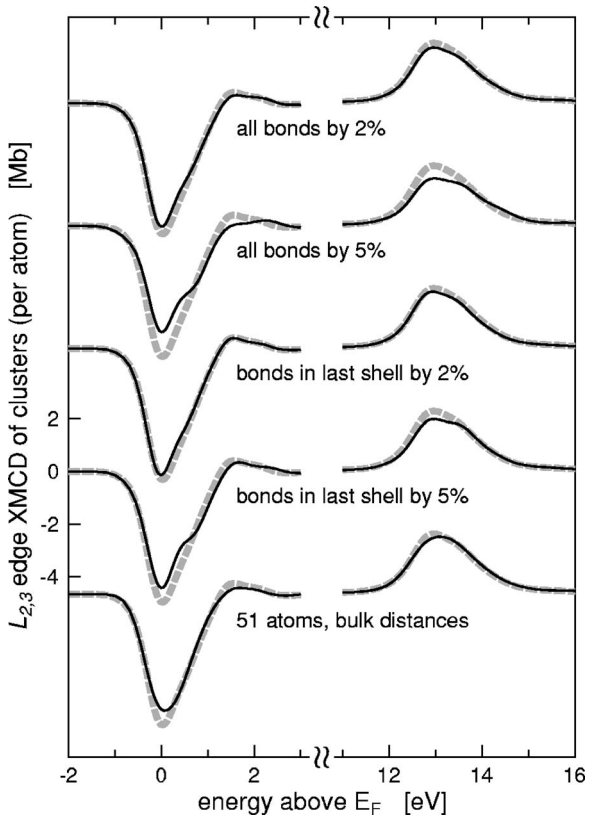

FIG. 9. $L_{2,3}$-edge XMCD of 27-atom clusters with contracted bond lengths. The type and magnitude of contraction is indicated at each curve. A spectrum of a nondeformed 51-atom cluster is shown at the bottom. Dashed thick gray lines represent the spectrum of a nondeformed 27-atom cluster in each subgraph.

the solid and dash-dotted lines in the two upper graphs of Fig. 8).

VI. EFFECT OF CONTRACTING THE BOND LENGTHS

It is difficult to estimate beforehand how bond lengths will be changed in clusters: some studies indicate that bond lengths in clusters decrease while opposite tendencies were observed by others.[83] *Ab initio* modeling of free Fe clusters suggests that some interatomic distances decrease while other increase.[28] In order to cover various situations, we investigate here two types of deformation. The first type is a uniform contraction of all interatomic distances. In the second case, only atoms of the outermost shell are moved inwards so that their nearest-neighbor distances are decreased. Contractions by 2% and 5% are considered for both types—these values are consistent with several previous studies.[24,28,84]

Studying the effect of bond length contraction is restricted to a 27-atom cluster in this study. The results are summarized in Fig. 9 ($L_{2,3}$ edge) and Fig. 10 (K edge). The two upper curves stand for XMCD spectra of clusters with all bonds uniformly contracted; the two curves below represent clusters with only the outermost shell contracted. Spectra of a nondeformed 27-atom cluster are shown in each subgraph by dashed thick gray lines for comparison. Spectrum of a nondeformed 51-atom cluster is shown at the bottom. The corresponding values of average d components of magnetic moments are summarized in Table II.

The changes induced upon XMCD spectra by contracting bond lengths are mostly only quantitative. The general trends are not surprising. Larger contractions lead to larger changes in XMCD spectra. Decreasing bond lengths for all atoms affects the spectra more than decreasing bond lengths only in the last shell. Smaller interatomic distances mean also smaller magnetization (Table II), in agreement with intuitive expectation. So to a certain degree, contracting the bond lengths has a similar effect as increasing the cluster size. We do not expect that this would obscure the cluster size effect altogether: the properties of clusters of all sizes would be, namely, affected by the effect of bond length contraction in a similar degree.

Some effects of varying the bond lengths are specific to a particular edge. Large contractions introduce a fine structure in the L_3-edge XMCD peak (Fig. 9). At the K edge, increasing the cluster size has a significantly larger effect than varying bond lengths (all XMCD curves for a 27-atom cluster have two oscillations between 5 eV and 11 eV while for 51-atom cluster there is only one oscillation in the same region).

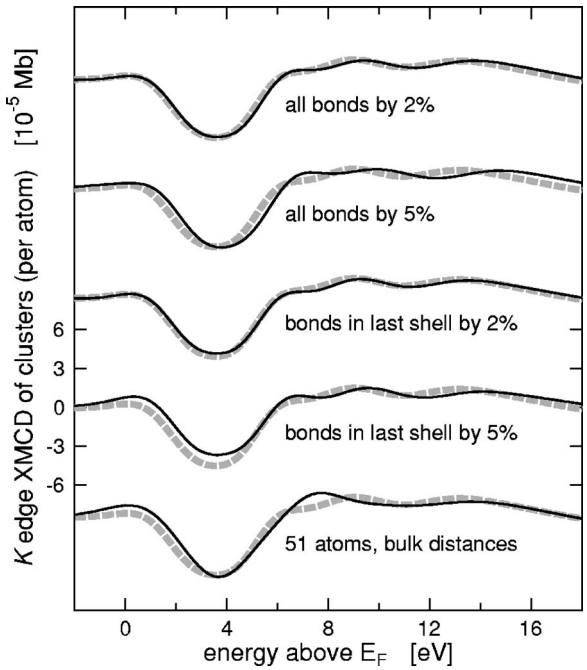

FIG. 10. *K*-edge XMCD of 27-atom clusters with contracted bond lengths. The meaning of the lines in the same as in Fig. 9.

VII. SUMMARY

The difference between the electronic and magnetic properties of Fe clusters and of a Fe crystal is reflected by the difference in their XMCD spectra. This difference is more significant for the *K*-edge than for the $L_{2,3}$-edge spectra. The *L*-edge XMCD spectra of the clusters differ from the bulk spectrum quantitatively through higher intensities of the dominant XMCD peaks. The *K*-edge XMCD of clusters exhibits different shapes of the spectral curves when compared to the bulk. A small positive hump just after the main L_3 peak and the absence of an intensive positive peak at the onset of the *K* edge may serve as markers of the difference between clusters and the bulk in XMCD spectra. As a general rule, the XANES spectra of clusters differ at the *K* edge from spectra of their bulk counterparts significantly, while at the $L_{2,3}$ edge this difference is only quantitative. Contracting the bond lengths affects XMCD spectra only quantitatively.

TABLE II. Influence of contracting the bond lengths on the magnetic properties of a 27-atom cluster. The first column specifies the type of bonds contraction, the second column shows the average *d* component of the spin magnetic moment $\mu_{\mathrm{spin}}^{(d)}$, the third column shows the average of ratios $\mu_{\mathrm{spin}}^{(d)}/n_h^{(d)}$, and the fourth column contains the average *d* component of the orbital magnetic moment $\mu_{\mathrm{orb}}^{(d)}$. Data for 27-atom and 51-atom clusters with bulk interatomic distances are included for comparison. Magnetic moments are in μ_B.

Cluster type	$\mu_{\mathrm{spin}}^{(d)}$	$\mu_{\mathrm{spin}}^{(d)}/n_h^{(d)}$	$\mu_{\mathrm{orb}}^{(d)}$
27 atoms, bulk distances	2.82	0.823	0.125
All distances by 2%	2.67	0.790	0.097
All distances by 5%	2.47	0.735	0.087
Last shell bonds by 2%	2.66	0.796	0.103
Last shell bonds by 5%	2.64	0.795	0.092
51 atoms, bulk distances	2.62	0.784	0.075

ACKNOWLEDGMENTS

This work was supported by Grant No. 202/04/1440 of the Grant Agency of the Czech Republic. The research in the Institute of Physics AS CR was supported by Project No. AV0Z-10100521 of the Academy of Sciences of the Czech Republic. Additionally, support by the Deutsche Forschungsgemeinschaft within the Schwerpunktprogramm 1153 "Cluster in Kontakt mit Oberflächen: Elektronenstruktur und Magnetismus" and by BMBF Project No. 05KS4WMB/2 is gratefully acknowledged.

*Electronic address: sipr@fzu.cz; URL: http://www.fzu.cz/~sipr
†Electronic address: Hubert.Ebert@cup.uni-muenchen.de; URL: http://olymp.phys.chemie.uni-muenchen.de/ak/ebert/index_eng.html

[1] K. W. Edmonds, C. Binns, S. H. Baker, S. C. Thornton, C. Norris, J. B. Goedkoop, M. Finazzi, and N. B. Brookes, Phys. Rev. B **60**, 472 (1999).
[2] P. Ohresser, G. Ghiringhelli, O. Tjernberg, N. B. Brookes, and M. Finazzi, Phys. Rev. B **62**, 5803 (2000).
[3] K. W. Edmonds, C. Binns, S. H. Baker, M. J. Maher, S. C. Thornton, O. Tjernberg, and N. B. Brookes, J. Magn. Magn. Mater. **231**, 113 (2001).
[4] C. Binns, S. H. Baker, M. J. Maher, S. Louch, S. C. Thornton, K. W. Edmonds, S. S. Dhesi, and N. B. Brookes, Phys. Status Solidi A **189**, 339 (2002).
[5] J. T. Lau, A. Föhlisch, R. Nietubyc, M. Reif, and W. Wurth, Phys. Rev. Lett. **89**, 057201 (2002).
[6] J. T. Lau, A. Föhlisch, M. Martins, R. Nietubyc, M. Reif, and W. Wurth, New J. Phys. **4**, 98 (2002).
[7] R. Wienke, G. Schütz, and H. Ebert, J. Appl. Phys. **69**, 6147 (1991).
[8] B. T. Thole, P. Carra, F. Sette, and G. van der Laan, Phys. Rev. Lett. **68**, 1943 (1992).
[9] G. Schütz, M. Knülle, and H. Ebert, Phys. Scr. **T49**, 302 (1993).
[10] P. Carra, B. T. Thole, M. Altarelli, and X. Wang, Phys. Rev. Lett. **70**, 694 (1993).
[11] I. M. L. Billas, J. A. Becker, A. Chatelain, and W. A. de Heer, Phys. Rev. Lett. **71**, 4067 (1993).
[12] I. M. L. Billas, A. Chatelain, and W. A. de Heer, J. Magn. Magn. Mater. **168**, 64 (1997).
[13] Z. Šljivančanin and A. Pasquarello, Phys. Rev. Lett. **90**, 247202 (2003).
[14] F. Federmann, O. Björneholm, A. Beutler, and T. Möller, Phys. Rev. Lett. **73**, 1549 (1994).
[15] S. Kakar, O. Björneholm, J. Weigelt, A. R. B. de Castro, L. Tröger, R. Frahm, T. Möller, A. Knop, and E. Rühl, Phys. Rev.

Lett. **78**, 1675 (1997).
[16] K. Nagaya, M. Yao, T. Hayakawa, Y. Ohmasa, Y. Kajihara, M. Ishii, and Y. Katayama, Phys. Rev. Lett. **89**, 243401 (2002).
[17] P. A. Montano, J. Zhao, M. Ramanathan, G. K. Shenoy, and W. Schulze, Z. Phys. D: At., Mol. Clusters **12**, 103 (1989).
[18] E. K. Parks, B. J. Winter, T. D. Klots, and S. J. Riley, J. Chem. Phys. **96**, 8267 (1992).
[19] M. Pellarin, B. Baguenard, J. L. Vialle, J. Lermé, M. Broyer, J. Miller, and A. Perez, Chem. Phys. Lett. **217**, 349 (1994).
[20] E. K. Parks, G. C. Nieman, L. G. Pobo, and S. J. Riley, J. Chem. Phys. **88**, 6260 (1988).
[21] L. S. Wang, H. S. Cheng, and J. Fan, J. Chem. Phys. **102**, 9480 (1995).
[22] S. Bouarab, A. Vega, J. A. Alonso, and M. P. Iñiguez, Phys. Rev. B **54**, 3003 (1996).
[23] J. Guevara, F. Parisi, A. M. Llois, and M. Weissmann, Phys. Rev. B **55**, 13283 (1997).
[24] O. Diéguez, M. M. G. Alemany, C. Rey, P. Ordejón, and L. J. Gallego, Phys. Rev. B **63**, 205407 (2001).
[25] P. Ballone and R. O. Jones, Chem. Phys. Lett. **233**, 632 (1995).
[26] G. M. Pastor, J. Dorantes-Dávila, and K. H. Bennemann, Phys. Rev. B **40**, 7642 (1989).
[27] A. N. Andriotis and M. Menon, Phys. Rev. B **57**, 10069 (1998).
[28] A. V. Postnikov, P. Entel, and J. M. Soler, Eur. Phys. J. D **25**, 261 (2003).
[29] O. Šipr, M. Košuth, and H. Ebert, Phys. Rev. B **70**, 174423 (2004).
[30] S. H. Vosko, L. Wilk, and M. Nusair, Can. J. Phys. **58**, 1200 (1980).
[31] V. Ozoliņš and M. Körling, Phys. Rev. B **48**, R18304 (1993).
[32] M. Battocletti, H. Ebert, and H. Akai, Phys. Rev. B **53**, 9776 (1996).
[33] I. Galanakis, S. Ostanin, M. Alouani, H. Dreysse, and J. M. Wills, Phys. Rev. B **61**, 599 (2000).
[34] R. Hafner, D. Spišák, R. Lorenz, and J. Hafner, Phys. Rev. B **65**, 184432 (2002).
[35] H. Ebert, The Munich SPR-KKR package, version 2.1, http://olymp.cup.uni-muenchen.de/ak/ebert/SPRKKR.
[36] H. Ebert, in *Electronic Structure and Physical Properties of Solids*, edited by H. Dreyssé, Vol. 535 of *Lecture Notes in Physics* (Springer, Berlin, 2000), p. 191.
[37] M. Cook and D. A. Case, The XASW program package, Quantum Chemistry Program Exchange, Indiana University, Bloomington, 1980.
[38] O. Šipr and A. Šimůnek, J. Phys.: Condens. Matter **13**, 8519 (2001).
[39] O. Šipr and H. Ebert, Czech. J. Phys. **53**, 55 (2003).
[40] P. Bruno, Phys. Rev. B **39**, R865 (1989).
[41] T. Fujikawa and S. Nagamatsu, Jpn. J. Appl. Phys., Part 1 **41**, 2005 (2002).
[42] T. Fujikawa and S. Nagamatsu, J. Electron Spectrosc. Relat. Phenom. **129**, 55 (2003).
[43] U. von Barth and G. Grossmann, Phys. Rev. B **25**, 5150 (1982).
[44] E. A. Stern and J. J. Rehr, Phys. Rev. B **27**, 3351 (1983).
[45] P. A. Lee and G. Beni, Phys. Rev. B **15**, 2862 (1977).
[46] R. Brydson, J. Bruley, and J. M. Thomas, Chem. Phys. Lett. **149**, 343 (1988).
[47] O. Šipr, P. Machek, A. Šimůnek, J. Vackář, and J. Horák, Phys. Rev. B **56**, 13151 (1997).
[48] R. Wu, D. Wang, and A. J. Freeman, J. Magn. Magn. Mater. **132**, 103 (1994).
[49] C. Brouder, M. Alouani, and K. H. Bennemann, Phys. Rev. B **54**, 7334 (1996).
[50] M. Alouani, J. M. Wills, and J. W. Wilkins, Phys. Rev. B **57**, 9502 (1998).
[51] E. Tamura, J. van Ek, M. Fröba, and J. Wong, Phys. Rev. Lett. **74**, 4899 (1995).
[52] J. Schwitalla and H. Ebert, Phys. Rev. Lett. **80**, 4586 (1998).
[53] E. L. Shirley, Phys. Rev. Lett. **80**, 794 (1998).
[54] A. L. Ankudinov, A. I. Nesvizhskii, and J. J. Rehr, Phys. Rev. B **67**, 115120 (2003).
[55] F. A. Shamma, M. Abbate, and J. C. Fuggle, in *Unoccupied Electron States*, edited by J. C. Fuggle and J. E. Inglesfield (Springer Verlag, Berlin, 1992), p. 347.
[56] J. E. Müller, O. Jepsen, and J. W. Wilkins, Solid State Commun. **42**, 365 (1982).
[57] M. Benfatto, S. Della Longa, and C. R. Natoli, J. Synchrotron Radiat. **10**, 51 (2003).
[58] A. L. Ankudinov and J. J. Rehr, Phys. Rev. B **52**, 10214 (1995).
[59] A. L. Ankudinov and J. J. Rehr, Phys. Rev. B **56**, R1712 (1997).
[60] C. T. Chen, Y. U. Idzerda, H. J. Lin, N. V. Smith, G. Meigs, E. Chaban, G. H. Ho, E. Pellegrin, and F. Sette, Phys. Rev. Lett. **75**, 152 (1995).
[61] R. Wu, D. Wang, and A. J. Freeman, Phys. Rev. Lett. **71**, 3581 (1993).
[62] T. Huhne and H. Ebert, Solid State Commun. **109**, 577 (1999).
[63] J. Kuneš and P. M. Oppeneer, Phys. Rev. B **67**, 024431 (2003).
[64] H. Ebert, Rep. Prog. Phys. **59**, 1665 (1996).
[65] G. D. Waddill, J. G. Tobin, and D. P. Pappas, J. Appl. Phys. **73**, 6748 (1993).
[66] K. Amemiya, S. Kitagawa, D. Matsumura, T. Yokoyama, and T. Ohta, J. Phys.: Condens. Matter **15**, S561 (2003).
[67] S. Pizzini, A. Fontaine, E. Dartyge, C. Giorgetti, F. Baudelet, J. P. Kappler, P. Boher, and F. Giron, Phys. Rev. B **50**, 3779 (1994).
[68] H. Ebert, P. Strange, and B. L. Gyorffy, J. Appl. Phys. **63**, 3055 (1988).
[69] H. J. Gotsis and P. Strange, J. Phys.: Condens. Matter **6**, 1409 (1994).
[70] J. I. Igarashi and K. Hirai, Phys. Rev. B **50**, 17820 (1994).
[71] G. Y. Guo, J. Phys.: Condens. Matter **8**, L747 (1996).
[72] H. Ebert, Solid State Commun. **100**, 677 (1996).
[73] H. Ebert, V. Popescu, D. Ahlers, G. Schütz, L. Lemke, H. Wende, P. Srivastava, and K. Baberschke, Europhys. Lett. **42**, 295 (1998).
[74] O. K. Andersen, Phys. Rev. B **12**, 3060 (1975).
[75] U. von Barth and L. Hedin, J. Phys. C **5**, 1629 (1972).
[76] R. Wu and A. J. Freeman, Phys. Rev. Lett. **73**, 1994 (1994).
[77] E. Martínez, R. C. Longo, R. Robles, A. Vega, and L. J. Gallego, Phys. Rev. B **71**, 165425 (2005).
[78] O. Šipr and H. Ebert, Phys. Scr. **T115**, 110 (2005).
[79] A. P. Cracknell, J. Phys. C **2**, 1425 (1969).
[80] G. Y. Guo, H. Ebert, W. M. Temmerman, and P. J. Durham, Phys. Rev. B **50**, 3861 (1994).
[81] A. L. Ankudinov and J. J. Rehr, Phys. Rev. B **51**, 1282 (1995).
[82] H. Ebert, V. Popescu, and D. Ahlers, Phys. Rev. B **60**, 7156 (1999).
[83] A. Traverse, New J. Chem. **22**, 677 (1998).
[84] H. Purdum, P. A. Montano, G. K. Shenoy, and T. Morrison, Phys. Rev. B **25**, 4412 (1982).